Journal of Theoretical and Applied Information Technology
30th June 2019. Vol.97. No 12

ISSN: 1992-8645 www.jatit.org E-ISSN: 1817-3195

THE EFFECT OF STATOR WINDING PARAMETER DESIGN TO THE MAGNETIC FLUX CHARACTERISTICS IN HIGH-SPEED MOTOR APPLICATIONS

[1]WAWAN PURWANTO, [2]HASAN MAKSUM, [3]TOTO SUGIARTO, [4]M NASIR, [5]MARTIAS, [6]FAHMI RIZAL

[1-6]Automotive Department, Engineering Faculty, Universitas Negeri Padang, West Sumatera, Indonesia 25131

E-mail: wawan5527@ft.unp.ac.id

ABSTRACT

The purposed of this research is an evaluation of magnetic flux characteristics for the high-speed motors in different stator winding topologies. This is essentiality for developing a stator arrangement with lower stator leakage and higher magnetic flux linkage. The topologies of stator parameters are generated using Hooke-Jeeves optimization, Taguchi method, and response surface methodology (RSM). The influence of stator winding topologies obtained from design optimizations are evaluated by using flux linkage finite element analysis. The stator leakage and magnetic flux resulting from finite element are verified with prototype motor model produced by Taguchi method optimization. The result confirm that proposed designs reduce stator leakage reactance and increase magnetic flux linkage than initial design had. A comparing of the optimize design and the prototype experimental results confirm the reasonable of the suggested motor model.

Keywords: *Hooke-Jeeves Optimization, Magnetic Flux Linkage, Response Surface Methodology, Taguchi Method, Stator Parameters*

1. INTRODUCTION

High-speed spindle motors have been widely used in various industry applications such as machine tools, compressors, and frictions welding units because they provide high efficiency, high power density, and excellent dynamic properties [7-9, 11, 20]. Generally, the performance of the spindle motor is largely determined by the value of the leakage reactance, which has substantial influence on magnetic flux linkage from the stator to the rotor. Hence, magnetic flux linkage and stator leakage reactance have been widely investigated by researchers to improve motor performance [2, 5, 6, 12-14, 16, 18].

With advances in powerful computing facilities, more accurate investigations of magnetic flux linkage and stator leakage reactance are desired. [2] investigated the flux linkage in a submersible motor. They constructed finite element models with various stator slot types to measure the slot flux linkage. [7] subsequently investigated the stator leakage reactance, flux linkage, and iron loss in a squirrel cage induction motor. [14] and [5] have developed energy conservation methods to examine the effects of stator leakage reactance on magnetic flux linkage. Experimental investigations of the stator leakage reactance effect on motor performance have been performed in [12,16,18,23], in which the theoretical predictions regarding the stator leakage reactance effect on motor performance were experimentally verified. The results indicated that the theoretical predictions and experimental data exhibited excellent agreement.

Studies [4,13,15] using field analysis computation in semi-closed stator slots has accurately predicted flux linkage. Combinations of finite element analysis (FEA) methods have been reported that use Maxwell's equations combined with FEA [17], equivalent circuits, and linkage field analysis with FEA [3,10]. Magnetic flux distributions in the stator winding are influenced by the varying reactance in the stator and rotor topologies as well as the core saturation. Furthermore, stator leakage is a crucial component of the total flux leakage. Stator leakage reactance has various components, including coil (winding), slots, and air-gap terms [10, 24]. Nearly all past research on the improvement of the motor performance through the design and control of the

ISSN: 1992-8645 www.jatit.org E-ISSN: 1817-3195

stator parameters has suggested method to reduce stator leakage reactance and increase magnetic flux linkage. This present study investigates magnetic flux linkage in stator windings with difference topologies generated from Hooke-Jeeves optimization, Taguchi methods, and RSM.

The purpose of this study is to produce a spindle motor suitable for use in machine tool applications with a speed reaching 21000 rpm with high magnetic flux linkage, torque, and efficiency. Magnetic flux linkage analysis was developed to evaluate the stator winding design. To validate the simulation results, a test was conducted by using the proposed design of Taguchi method prototype motor are described in [19].

2. MAGNETIC FLUX LINKAGE ANALYSIS

To evaluate the flux linkage characteristics of the stator winding designs, three analyses are described, namely flux linkage FEA, stator leakage reactance and flux linkage analysis, and analysis of stator leakage and magnetic flux linkage effects on the torque of spindle motors.

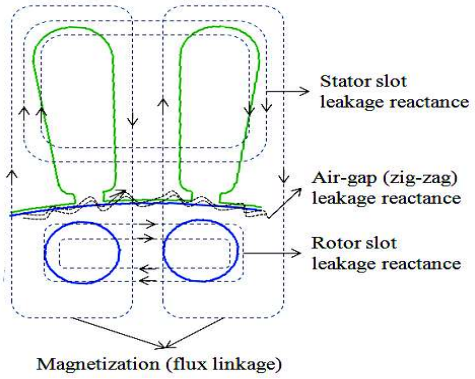

Figure 1. Flux leakage and linkage in the stator and rotor

2.1 Flux Linkage FEA

A stator winding current produces a magnetic flux in the stator winding. Subsequently, the magnetic flux is transferred from the stator to the rotor. However, presence of stator leakage reactance causes minor flux leakage is observed at the slots, air-gaps (zig-zag leakage), and end turns winding (Figure 1). The magnetic flux in the vector potential A can be expressed by (1), a two-dimensional Maxwell equations for magnetic potential FEA (2), and flux computation FEA by a Euler equation of the nonlinear energy function (3) [3]:

$$A = \frac{(\mu \div 4\pi)\varphi dL_i}{r} \quad (1)$$

$$\frac{\partial}{\partial x}\left(\frac{1}{\mu_0}\frac{\partial A}{\partial x}\right)+\frac{\partial}{\partial y}\left(\frac{1}{\mu_0}\frac{\partial A}{\partial y}\right)-\sigma\frac{dA}{dt}+J=0 \quad (2)$$

$$F=\iint_R\left(\int_0^B vb\ db\right)dx\ dy-\iint_R JA\,dx\,dy \quad (3)$$

where A is the magnetic potential, μ_0 is the permeability of the magnetic material, r is the radius of the homogeneous conductor, L_i is the stator length, J is the current density at time t, b is the magnetic field, and σ is the equivalent conductivity of the rotor bar. The flux which is linked to the number of winding turns can be expressed according to flux density B and the area of the stator windings as follows:

$$\phi = \int B.dS \quad (4)$$

The flux is expressed as follows:

$$\phi = \int (\nabla x\, A) dS \quad (5)$$

If the vector of the potential magnetic flux on the right and left sides of the winding turns are denotes as A_R and A_L, and N_s is the number of stator slot, then the total flux linkage can be calculated as follows:

$$\psi = N_s\phi = N_s L_i (A_R - A_L) \quad (6)$$

2.2 Stator flux linkage and stator leakage reactance analysis

Stator flux must cross the air gap and enclose the rotor conductor (bar), establishing flux linkage. The slot flux leakage crosses the slot width at various slot heights. Each flux line is generated by currents induced in the slots of the stator conductor. Considering the total useful slot geometry, the total flux linkage is expressed as:

$$\psi = \mu_o\left(\frac{hs_o}{bs_o}+\frac{2hs_1}{bs_1+bs_2}+\frac{hs}{bs_2}+\frac{3hs_1}{3bs_2}\right)L_i I_s \quad (7)$$

or

$$\psi = \mu_o L_i I_s S_o \quad (8)$$

where hs, hs_0, and hs_1 are the stator slot parameters, bs_0, bs_1, and bs_2 are the rotor slot parameters, I_s is the stator current, and S_o is the slot permeance ratio. Furthermore, the stator slots per phase are N_s/q, and the flux linkage of the phase winding is as follows:

$$\psi_{ps} = \mu_o L_i I_s S_o\left(\frac{N_s}{q}\right)\left(\frac{2qN_s}{N_s}\right)^2 \quad (9)$$

The stator leakage reactance (X_{ph}) per phase as follows [10]:

$$X_{ph} = \frac{\psi_{ps}}{I_s} = \mu_o L_i S_o\left(\frac{N_s}{q}\right)\left(\frac{2qN_s}{N_s}\right) \quad (10)$$

ISSN: 1992-8645 www.jatit.org E-ISSN: 1817-3195

where q is the number of stator slot per pole per phase, stator phase current closely related to the number of winding turns, wire diameter, and stator resistance. Eq. 10 shows the optimal stator phase current that produces the lowest stator leakage reactance per phase and the highest flux linkage of the phase winding [13, 17]. Furthermore, the magnetic flux linkage in the stator at the rated speed can be obtained through alternative equivalent circuit analysis as follows [2]:

$$\psi_s \sqrt{2} = \frac{\sqrt{2}\left|V_1 - I_s R_2\right|}{\omega_m} \tag{11}$$

2.3 Influence of the stator flux linkage and stator leakage reactance in the torque of a spindle motor

The influence of stator leakage reactance and magnetic flux linkage caused by the stator winding geometry was investigated by examining the maximum torque and torque-speed characteristics through an equivalent circuit analysis [2]. To make fair comparison, that the maximum torque and torque-speed characteristics are only defined and controlled by the stator leakage reactance, for a model at a given time, rotor geometry, rated voltage and frequency, and rated output power are all fixed. The maximum torque is influenced by the stator leakage reactance can be calculated as (12), and the torque-speed characteristics as (13), respectively.

$$T_{\max} = \frac{3p_1 V_1^2}{2\omega_m[R_1 + \sqrt{R_1^2 + (X_1 + C_m X_2)^2}]} \tag{12}$$

$$T_e = \frac{3p_i V_1^2 \frac{R_2}{s}}{\omega_m\left(R_1 + C_m \frac{R_2}{s}\right)^2 + (X_1 + X_2)} \tag{13}$$

where ω_m is the synchronous speeds, R_1 and R_2 are the stator and rotor resistance, X_1 and X_2 are the stator and rotor leakage reactance, C_m is the capacitor parameter, X_m is the magnetization reactance, and V_1 is representation of the phasor diagram of V_{ieq} and $Z_{ieq} = R_{1eq} + jX_{1eq}$, as follows:

$$V_1 = \left|\frac{jX_m V_{ieq}}{R_1 + j(X_1 + X_m)}\right| \qquad Z_{ieq} = \frac{jX_m(R_1 + jX_1)}{R_1 + j(X_1 + X_m)} \tag{14}$$

3. MATERIAL AND METHOD

Table 1. Spindle motor specifications

Parameter	Value
Inner diameter of stator (mm)	70
Outer diameter of stator (mm)	120
Length of the stator core (mm)	120
Outer diameter of rotor (mm)	69.3
Inner diameter of rotor (mm)	38
Number of stator/rotor slot	36/32

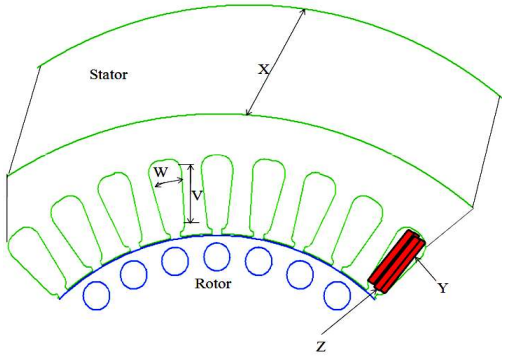

Figure 2. Definition of factors

In this study, an industrial spindle motor design, which had a rated output of 14 kW, four poles, a Δ connection, and 380 V, rotating at 21000 rpm with the general specifications listed in Table 1. An optimized stator winding geometry was based the rotor geometry of the current industrial spindle motor design. The optimal parameter definitions and design levels classification of those factors are corresponding to five design variables, denote as *V, W, X, Y,* and *Z* as shown in Figure 2. Each factor consists of five levels.The factor-level combinations are listed in Table 2.

A statistical analysis was applied for optimization [21, 22], as shown in Figure 3, with efficiency and torque as objective functions. The optimized stator winding was verified using FEA [1]. The optimal stator geometry design results are listed in Table 3. The prototype high-speed spindle motor was developed according to the proposed Taguchi method design results [19]. The stator material used was 35H250.

To make a fair comparison in this study, circular closed rotor slot type of squirrel cage was used for all stator designs. The circular closed rotor slots were designed by copper rotor bar and end ring conductor type. These features guided the magnetic flux from the stator to the rotor and reduced the eddy current loss, rotor resistance, and rotor slot leakage reactance. Thus, these features increased performance of the spindle motor.

ISSN: 1992-8645 www.jatit.org E-ISSN: 1817-3195

Table 2. Design levels classifications

Factors	Definitions	1	2	3	4	5
V	Useful slot area (*hs*) (mm)	5.5	6.5	7.5	8.5	9.5
W	Slot higher width (bs_2) (mm)	4	4.4	4.8	5.2	5.6
X	Stator length (*L*) (mm)	110	120	130	140	150
Y	Wire diameter (mm)	0.381	0.511	0.643	0.767	0.912
Z	Number of winding turns per slot (coil)	24	36	48	60	72

Table 3. Design optimization results

Parameter	Optimization results			
	Industrial design	Hooke-Jeeves	Taguchi method	RSM
Outer diameter of stator (mm)	120	120	120	120
Inner diameter of stator (mm)	70	70	70	70
Useful slot area (*hs*) (mm)	11	9.5	5.5	8
Slot higher width (bs_2) (mm)	5	5.6	5.6	4.8
Stator length (*L*) (mm)	120	140	110	120
Winding turn per slot (coil)	60	48	48	48
Wire Diameter (mm)	0.607	1.151	0.767	0.767

Table 4. The effect of stator parameter changes

Parameter	Industrial design	Hooke-Jeeves	Taguchi Method	RSM
Stator resistance (Ohm)	1.39	0.196	0.271	0.447
Stator current (A)	18.79	16.42	17.22	16.71
Stator current density (A/mm^2)	37.73	7.03	11.78	18.07
Stator thermal load (A^2/mm^3)	736.21	151.28	265.59	395.29
Copper loss stator winding (W)	580.51	158.76	241.46	374.71

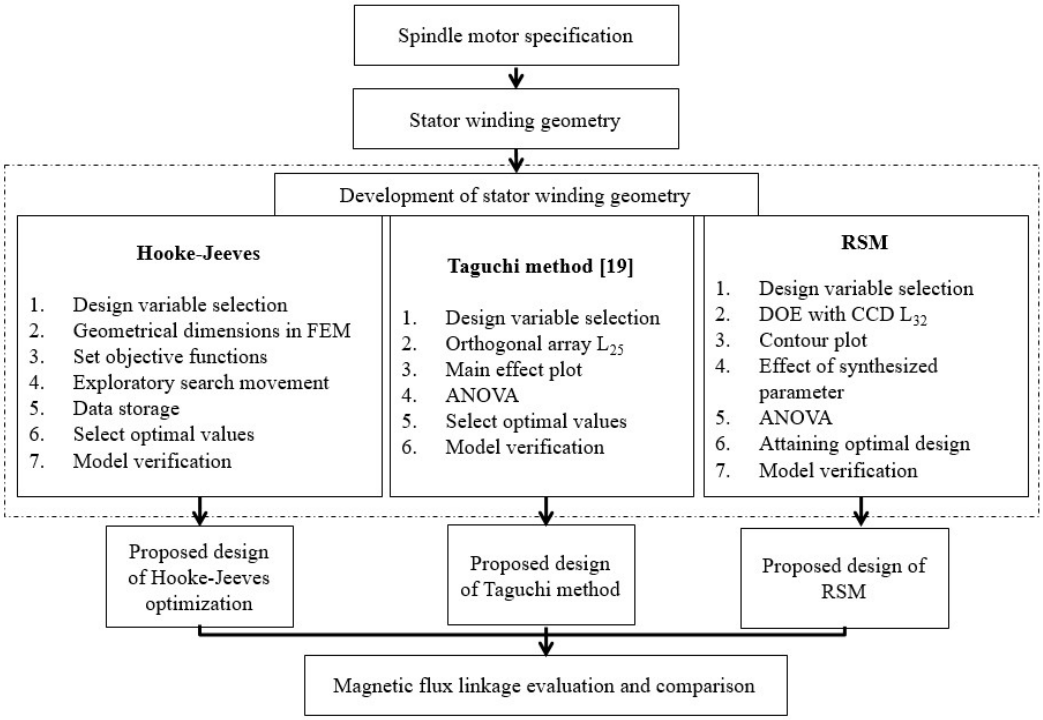

Figure 3. Flowchart of design optimization

ISSN: 1992-8645 www.jatit.org E-ISSN: 1817-3195

Table 5. ANOVA results

Factor	SS	d.f	Mean sq	F	Prob > F
V	0.1358	4	0.034	0.5694	0.701
W	0.4609	4	0.115	1.9321	0.269
X	1.4190	4	0.355	5.9476	0.056
Y	0.2533	4	0.063	1.0614	0.477
Z	126.3327	4	31.583	529.4986	0.00001
Error	0.2386	4	0.059		
Total	128.8404	24			

Table 6. The effect of difference number of winding turns per slot

Parameter	The number of winding turns per slot				
	72	60	48	36	24
Copper loss stator winding (W)	894.93	426.721	411.09	762.531	712.351
Iron core loss (W)	483.79	162.123	259.59	362.65	350.35
Magnetization current (A)	1.687	3.596	8.447	6.129	6.023
Stator teeth flux density (T)	0.991	1.139	1.163	1.152	1.121
Stator yoke flux density (T)	0.405	0.567	0.748	0.652	0.644
Air gap flux density (T)	0.376	0.512	0.612	0.563	0.551

Table 7. Simulation and experimental results

Parameter	Optimization and experimental results					
	Industrial design	Hooke-Jeeves	RSM	Taguchi method [19]	Experimental	Error (%)
Stator leakage reactance (Ohm)	2.967	2.746	2.351	2.291	2.353	2.63
Stator magnetic flux linkage (Wb)	0.082	0.086	0.085	0.085	0.084	1.19
Maximum torque (Nm)	3.12	7.56	7.65	7.86	7.86	0
Efficiency (%)	86.45	92.38	92.35	92.97	92.15	0.89

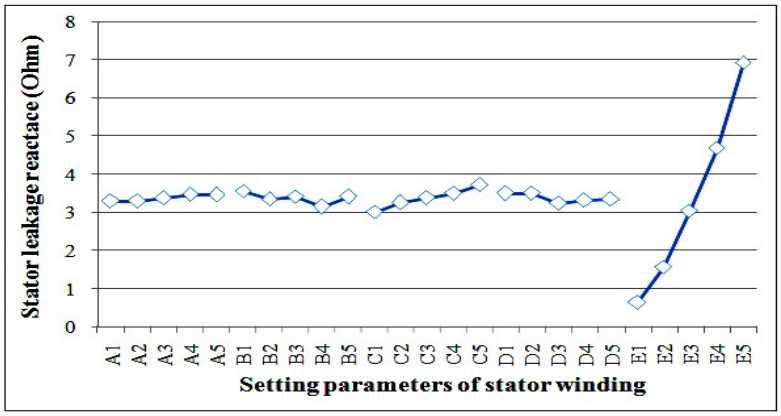

Figure 4. Main effect of stator leakage reactance

4. SIMULATION AND EXPERIMENTAL RESULTS

Table 3 shows that a short of the stator length requires small values of *hs, bs*$_2$, and wire diameter (such a design can be obtained through the Taguchi method). The proposed optimal design facilitates reducing the stator resistance through shortening the coil length and preventing an increasing in the stator current density, stator thermal load, as well as maintaining the flux density distribution equitable to the coil area. The slot cross-sectional area available for the number of winding turns per slot decreases, and consequently, the stator current density and copper losses to stator winding increase. Thus, an appropriate the wire diameter can be a solution.

ISSN: 1992-8645 www.jatit.org E-ISSN: 1817-3195

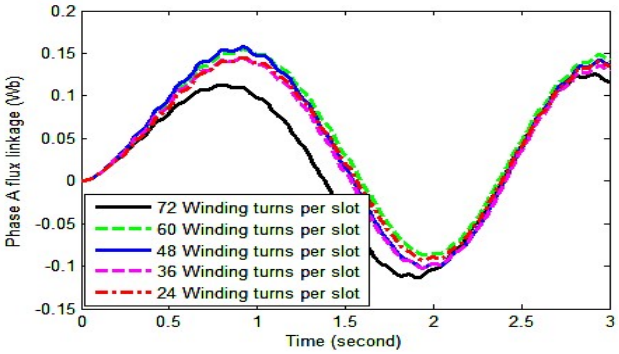

Figure 5. Flux linkage characteristics

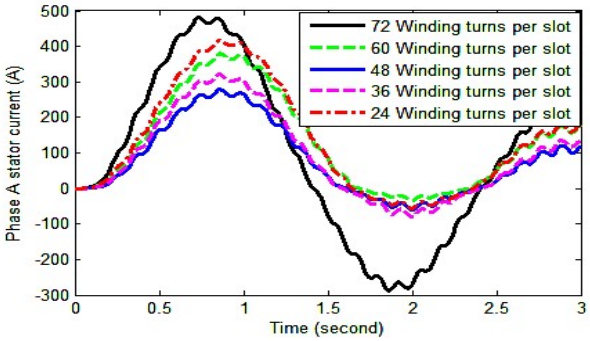

Figure 6. Stator current characteristics

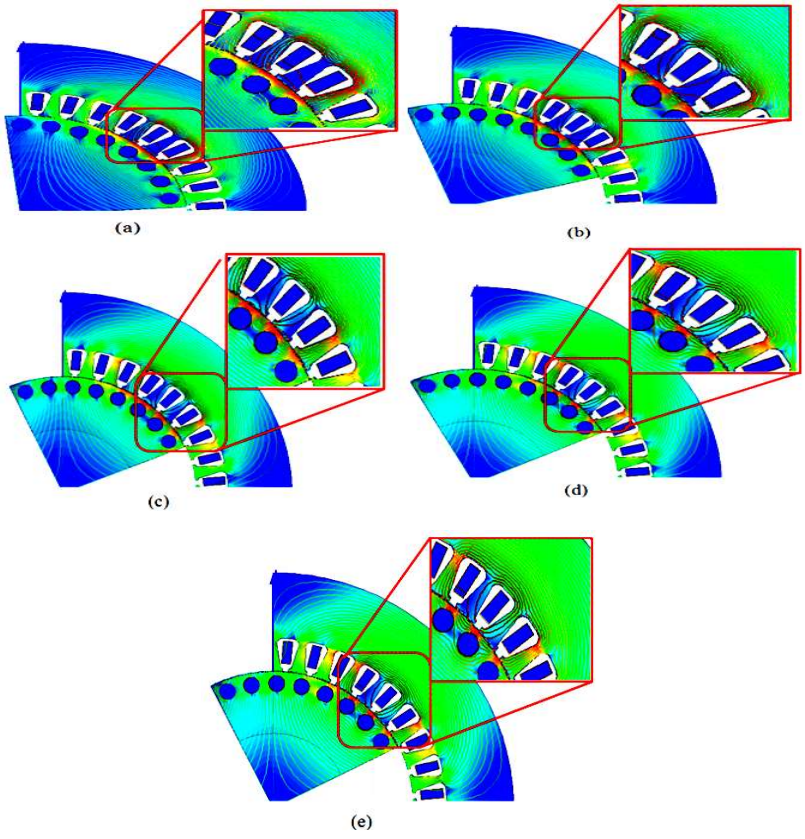

Figure 7. Flux density characteristics at difference the number of winding turns per slot, (a) 72, (b) 60, (c) 48, (d) 36, (e) 24.

ISSN: 1992-8645 www.jatit.org E-ISSN: 1817-3195

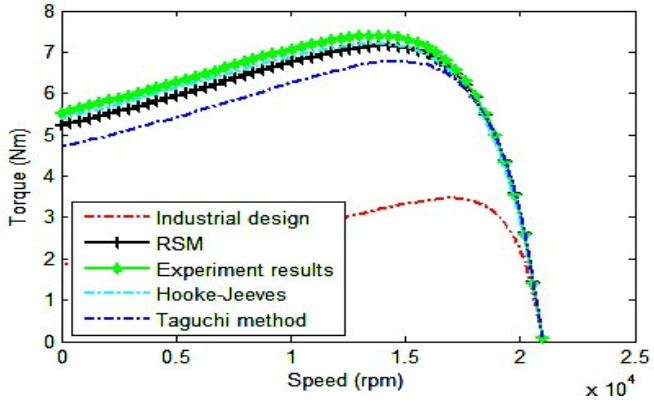

Figure 8. Torque-speed characteristics

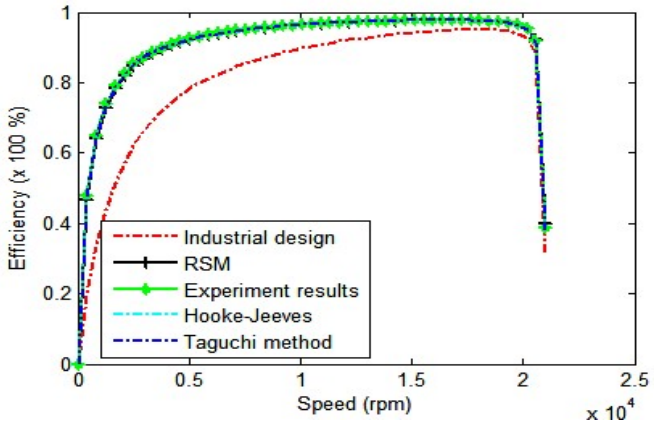

Figure 9. Efficiency characteristics

Table 8. Flux density characteristics

Parameter	Industrial design	Hooke-Jeeves	Taguchi method	RSM
Stator teeth flux density (T)	1.085	1.164	1.629	1.193
Stator yoke flux density (T)	0.555	0.746	0.755	0.791
Air gap Flux density (T)	0.415	0.517	0.618	0.581

The proposed designs of Hooke-Jeeves and RSM use appropriate wire diameters, as listed in Table 3. To investigate stator leakage reactance, analysis of variance was applied, and the results are listed in Table 4. The stator leakage reactance is greatly influenced by the number of winding turns per slot.

Furthermore, the influence of each factor on the stator leakage reactance is shown in Figure 4 and Table 5. Figure 5 represent higher the number of winding turns per slot produces higher stator leakage reactance and generates lower magnetic flux linkage. High stator current (Figure 6) in the stator winding turns to be stator slots leakage reactance, end turns leakage reactance, and air-gap leakage reactance.

High numbers of winding turns per slots and high stator leakage reactance also reduce the transfer of electromagnetic force from the stator winding to the rotor. This increases copper loss to stator winding and iron loss, but reduces magnetizing current, stator teeth flux density, stator yoke flux density, and air-gap flux density, as listed in Table 6.

The flux density characteristics for different the number of winding turns per slot are shown in Figure 7. Generally, high flux density can be found at the stator teeth and rotor surface.

Table 7 compares the data of the spindle motor between the industrial design, proposed optimal design (Hooke-Jeeves, Taguchi method [19], and RSM), and experimental results at speeds

ISSN: 1992-8645 www.jatit.org E-ISSN: 1817-3195

of 21000 rpm. The proposed optimal design produces lower leakage reactance and higher stator teeth flux density, stator yoke flux density, and air-gap flux density than does the current industrial design, as shown in Table 8. High magnetic flux density in the proposed optimized spindle motor induces increasing magnetic flux linkage from the stator to the rotor (Table 7), torque (Figure 8), and efficiency (Figure 9).

As shown in Table 7, the percentage errors between the simulation of the Taguchi method optimal design and the experimental measurement results at rotational speeds of 21000 rpm, the percentage errors in the stator leakage reactance and flux linkage are 2.63% and 1.19%, respectively.

A possible cause of the measured experimental values being higher than the simulated values is a slight change in the value for the stator slot geometry caused by the manufacturing process. Therefore, the high speed might have caused a high stator slot difference coefficient, leading to a high stator leakage reactance. Overall, the measured experimental results are in favorable agreement with the simulation results.

The essential characteristics regarding with this research is the stator slot geometry, winding turn per slots, and wire diameter that can generate current along the surface of the stator core with a sinusoidal distribution, than maintaining the magnetic flux in proportion to the coil area. The current concentration in the slots is caused by high frequency. It affects the concentration of the magnetomotive force (MMF) and causes current and torque ripple [4, 25].

The stator slots support for optimal supply current in the stator winding to produces a stronger magnetic flux distribution in the stator slot-air gap-rotor slot. Moreover, a stator teeth zone MMF is formed along the stator teeth-air gap-rotor teeth path. As well known, the magnetic field generated using the MMF distribution along the air gap weakens comparison with the magnetic field at the stator and rotor slot opening [15-18].

When the teeth zone is saturated, by the flux leakage, the induction distribution produced by the fundamental MMF waveform along the air-gap is distorted, causing higher flux pulsation density loss and iron loss. This is defined as Carter's coefficient and crucial for evaluating the performance of induction motor [3, 26].

When the spindle motor produces higher stator flux leakage, it is iron loss and magnetic flux leakage is also higher. Therefore, the efficiency and torque of the spindle motor reduces, as shown in Figures 8 and 9, causing the magnetic flux line distribution produced by the stator winding in the stator slots to split into zigzag leakage, slot leakage, end turns leakage, additional power loss, magnetizing reactance, and lower magnetizing current. Higher iron loss and stator slot leakage cause lower stator teeth and air gap flux density, as shown in Fig 10.

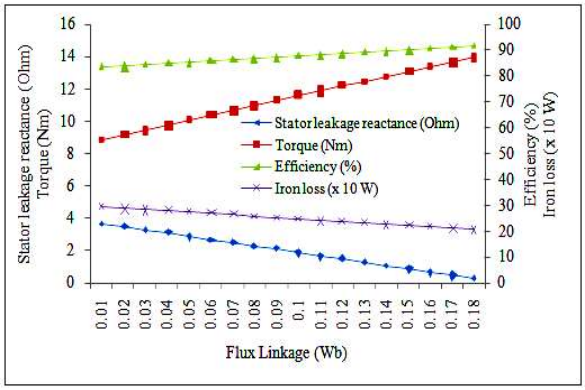

Figure 10. Relationship of stator slot leakage, iron loss, flux leakage to the torque and efficiency

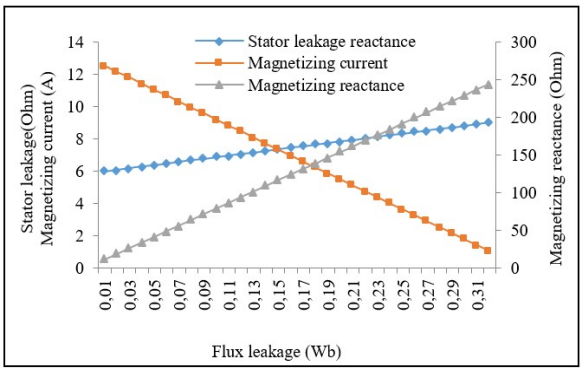

Figure 11. Effect of stator leakage, flux leakage with magnetizing current and magnetizing reactance

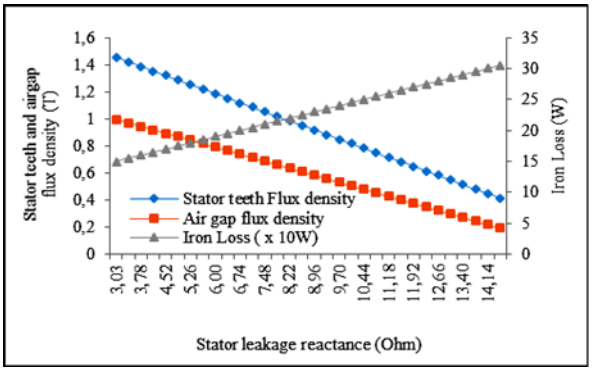

Figure 12. Effect of stator leakage reactance to the iron loss, stator teeth and air gap flux density

Journal of Theoretical and Applied Information Technology
30th June 2019. Vol.97. No 12

ISSN: 1992-8645 www.jatit.org E-ISSN: 1817-3195

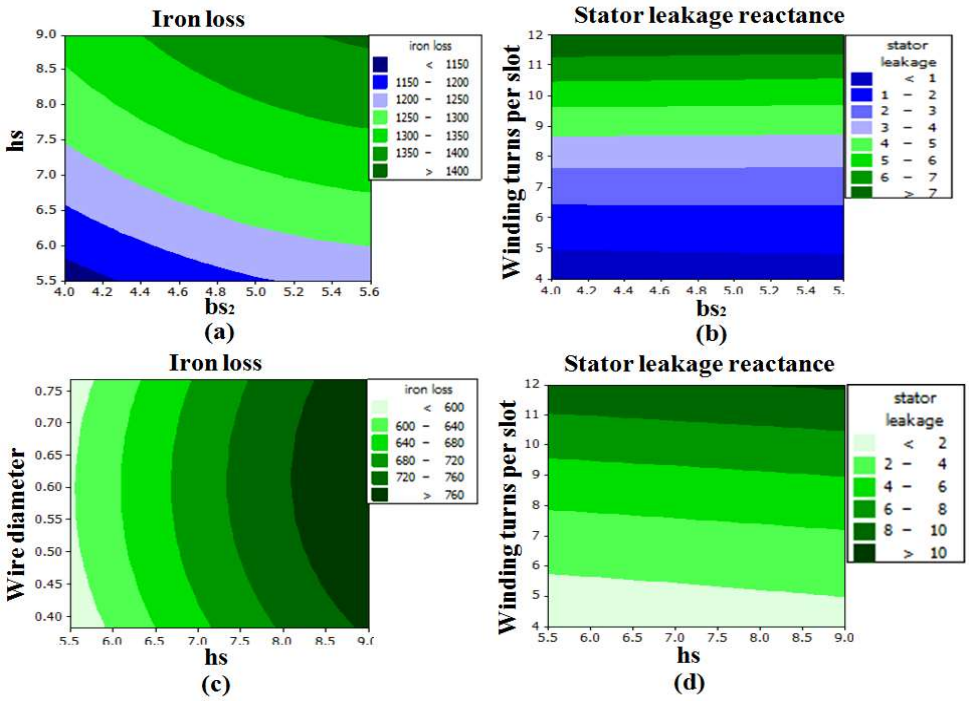

Figure 13. Contour plot for (a) hs and bs_2 with iron loss, (b) winding turn per slot and bs_2 with stator leakage, (c) wire diameter and hs with iron loss, (d) winding turn per slot and hs with winding turn per slot.

Figure 11 shows the characteristics of stator leakage, flux leakage with magnetizing current and magnetizing reactance. Lower stator leakage reactance and leakage, it is will produces higher magnetizing current and lower magnetizing reactance. Increase magnetizing reactance will increases travelling mmfs from stator winding to the rotor. Thereby increasing torque and efficiency as well as reduce the additional power loss, as shown in Figure 10.

Increasing the magnetizing current will cause an increase of the stator teeth and air gap flux density, as shown in Figure 12. Increase stator flux density affects the decrease of iron loss in the spindle motor, the induced current in the stator winding converted into higher mmfs in stator teeth and air gap flux density, thereby increasing power output.

The slot leakage distribution depend on notably on the slot geometry and less on the teeth and back core saturation, it is also depend on the current density distribution in the slot which may become non uniform due to eddy currents (skin effect) induced in the conductors in slot by their mmf leakage flux. Higher flux leakage may produce space flux density harmonic in the air gap, there will be both a stator and a rotor differential inductance.

The fundamental characteristics from this stydy is the optimal design of the stator slot geometry, winding turn per slots, and wire diameter that can generate current along the surface of the stator core with a sinusoidal distribution, than maintaining the magnetic flux in proportion to the coil area. When the teeth zone is saturated, by the flux leakage, the induction distribution produced by the fundamental MMF waveform along the air-gap is distorted, causing higher flux pulsation density loss and iron loss. Figure. 13 illustrates the plot of stator leakage and iron losses according to the stator parameter (RSM Results).

The Iron loss increases if parameter *hs* and bs_2 increase, and the high winding turns per slot and bs_2 cause higher stator leakage. The small wire diameter and *hs* can produce lower iron loss. To produce a low stator leakage, the winding turns per slot and *hs* should be lower. Moreover, *hs* parameter influences the iron loss. A higher *hs* parameter produces high stator leakage and iron loss, It is shows, to produce the best performance of spindle motors with lower iron loss and stator leakage reactance needed appropriate between

ISSN: 1992-8645 www.jatit.org E-ISSN: 1817-3195

stator parameter. The relationship among the stator leakage, magnetic flux leakage, iron loss, and efficiency can be derived. When the spindle motor produces higher stator leakage, it is iron loss and magnetic flux leakage is also higher. Therefore, the efficiency and torque of the spindle motor reduces. Causing the magnetic flux line distribution produced by the stator winding in the stator slots to split into zigzag leakage, slot leakage, end turns leakage, additional power loss, magnetizing reactance, and lower magnetizing current. Higher iron loss and stator slot leakage cause lower stator teeth and air gap flux density.

The result shows that shorting the stator length requires small values of *hs, bs*$_2$, and wire diameter (such a design can be obtained through the Taguchi method). The proposed optimal design facilitates reducing the stator resistance through shortening the coil length and preventing an increasing in the stator current density, stator thermal load, as well as maintaining the flux density distribution equitable to the coil area. The slot cross-sectional area available for the number of winding turns per slot decreases, and consequently, the stator current density and copper losses to stator winding increase. Thus, an appropriate wire diameter can be a solution.

5. CONCLUSION

To evaluate the flux linkage and iron loss characteristics of the stator winding designs, four analyses are described, namely flux linkage FEA, stator leakage reactance and flux linkage analysis, analysis of stator leakage and magnetic flux linkage effects on the torque of spindle motors, and iron loss analysis. In this study, several different topologies of stator winding geometry are obtained using Hooke-Jeeves optimization, Taguchi methods, and response surface methodology (RSM).

Compares the data of the spindle motor among the former design, proposed optimal design (Hooke-Jeeves, Taguchi method, and RSM), and experimental results at speeds of 21000 rpm. The proposed optimal design produces lower leakage reactance and higher stator teeth flux density, stator yoke flux density, and air-gap flux density than does the current former design. High magnetic flux density in the proposed optimized spindle motor induces increasing magnetic flux linkage from the stator to the rotor, torque and efficiency.

Some stator winding geometries, obtained using Hooke-Jeeves optimization, Taguchi methods, and RSM generated lower stator leakage reactance and greater magnetic flux linkage than does the current industrial design. Thus, the proposed design topology advances the field by offering greater than usual torque and efficiency. Comparison between simulation and experimental showed an overall percentage of error of approximately 2%. Furthermore, the proposed design topologies are reasonable for machine tool applications at speeds of 21.000 rpm.

ACKNOWLEDGEMENT

The researchers are greatful to rector of Universitas Negeri Padang for contributing in laboratory facilities for the experimental process in this research.

REFRENCES:

[1] Ansoft Maxwell user's guidance ver. 15. 2016. ANSYS. Inc, Southpointe, Canonsburg, USA.

[2] Bao X, Di C, and Fang. Y. "Analysis of slot leakage reactance of submersible motor with closed slots during starting transient operation". Journal of Electrical Engineering and Technology, Vol. 10, No.6, 2015, pp. 709-716.

[3] Boldea. I., and Nasar S.A. "The induction machines design handbook", CRC Press, 2nd edition. 2010.

[4] Cheaytani. J., Benabou A. A.Tounzi. M.Dessoude. L.Chevallier. and T.Henneron. End-region leakage fluxes and losses analysis of cage induction motors using 3-D finite-element method. IEEE Transactions on Magnetics. Vol. 51, No. 3, 2015, pp. 8101004

[5] Grop H., Soulard. J. and Persson H. "Stator slot leakage in AC-machines equipped with fractional conductor windings". International Conference of Electrical Machines and Systems (ICEMS), Tokyo, 2009, pp. 1-6.

[6] Hong. D.K., Choi J.H, Kim D.J, Chun Y.D, Woo B.C, and Koo D.H. "Development of a high speed induction motor for spindle systems". IEEE Transactions on Magnetic, Vol. 49, No. 7, 2013, pp. 4088-4091

[7] Hong G.Q., S.G. Ho. And G.J. Hwang. "Characteristics of a squirrel cage induction motor". IEE Proceedings B - Electric Power Applications, Vol. 138, No. 3, 1991, pp. 115-124.

[8] Hwang C.C., Hung S.S. Liu C.T. and Cheng S.P. "Optimal design of a high speed spm motor for machine tool applications". IEEE Transactions on Magnetic, Vol. 50, No. 1, 2014, pp. 1-4.

ISSN: 1992-8645 www.jatit.org E-ISSN: 1817-3195

[9] Kim, D.J. Hong. D.K. Choi J.H. Chun Y.D. Woo B.C. and D.H Koo. "An analytical approach for a high speed and high efficiency induction motor considering magnetic and mechanical problems". IEEE Transactions on Magnetic, Vol. 49, No. 5, 2013, pp. 2319-2322.

[10] Kirtley.J.L.Jr. Analytic design evaluation of induction machines. Massachusetts Institute of Technology. 2003.

[11] Menon P., Tong L.H, Zhijie L, and Ibrahim Y. "Robust Design of Spindle Motor: a Case Study". Reliability Engineering and System Safety, Vol. 75, 2002, pp. 313-319.

[12] Monjo L., Corcoles F. and Pedra J. "Saturation effects on torque- and current–slip curves of squirrel-cage induction motors". IEEE Transactions on Energy Conversion, Vol. 28, No. 1, pp. 243-254.

[13] Nishihama. K., Ide K. H.Mikami. T.Fujigaki. and S.Mizutani. "Starting torque analysis of cage induction motor using permeance model considering magnetic saturation by leakage flux". International Conference of Electrical Machines and Systems (ICEMS) Tokyo, 2009, pp.1-6.

[14] Pyrhonen J., Jokinen. T. and Hrabovcova V. "Design of Rotating Electrical Mechines". John Wiley& Sons, Ltd. 2008.

[15] Rui. Z., li L.G. Jing W.Q. Hui F.G. and G.X.Wen. "Leakage field computational analysis of closed slot motor based on ANSOFT". 17th International Conference on Electrical Machines and Systems (ICEMS), Hangzhou, China, 2014. pp. 1963-1965.

[16] Sudhoff. S.D., Aliprantis. D.C. Kuhn B.T. and P. L.Chapman. "Experimental characterization procedure for use with an advanced induction machine model". IEEE Transactions on Energy Conversion Vol. 18, No. 1, 2003, pp. 48-56.

[17] Tessarolo. A. "Leakage field analytical computation in semi closed slots of unsaturated electric machines". IEEE Transactions on Energy Conversion, Vol. 30, No. 2, 2015, pp. 431-440.

[18] Tuovinen T., Hinkkanen. M. and Luomi. J. "Modeling of saturation due to main and leakage flux interaction in induction machines". IEEE Transactions on Industry Applications, Vol. 46, No. 3, 2010, pp. 937-945.

[19] W. Purwanto. and S. C.T Jerry. "Improving the performance of high-speed spindle motor for machine tool applications". Asia Life Sciences, Vol. 25, No. 2, 2016, pp. 675-689.

[20] Williamson, S. and McClay. C.I. "Optimization of the geometry of closed rotor slots for cage induction motors". IEEE Transactions on Industry Applications, Vol. 32, No. 3, 1996, pp. 560-568.

[21] S.Slama, A. Errachdi, M. Benrejeb. "Adaptive PID controller based on neural networks for mimo nonlinear systems". Journal of Theoretical and Applied Information Technology, Vol. 97, No. 2, 2019, pp.361-371.

[22] H. K. Fatlawi, A. F. H. Alharan, N. S. Ali. "An efficient hybrid model for reliable classification of high dimensional data using k-means clustering and bagging ensemble classifier". Journal of Theoretical and Applied Information Technology. Vol. 96, No. 24, 2018, pp. 8379-8398.

[23] W. Purwanto, Risfendra, D. Fernandez, D. S. Putra, and T. Sugiarto. "Design and comparison of five topologies rotor permanent magnet synchronous motor for highspeed spindle applications". International Journal of GEOMATE, Vol. 13, No. 40, 2017, pp. 148-154.

[24] W. Purwanto, Risfendra, D. S. Putra. "Effect of Stator Slot Geometry on High Speed Spindle Motor Performance". 2018 International Conference on Information and Communications Technology (ICOIACT). Yogyakarta, 6-7 March 2018, pp. 560-564.

[25] K.W. Lee, D.S. Hyun, and E.J. Wiedenbrug, "Detection of stator-slot magnetic wedge failures for induction motors without disassembly", IEEE Trans. Industry Applications, Vol. 50, No. 4, 2014, pp. 2410-2419,

[26] W. Stephen, and C. I. McClay, "Optimization of the geometry of closed rotor slots for cage induction motors", IEEE Trans. on Industry Applications, Vol. 32, No. 3, 1996, pp. 560-568.